

Observation of $D_s^+ \rightarrow \bar{K}^0 K^+$ and $D_s^+ \rightarrow \bar{K}^{*0} K^+$ and an Upper Limit on $D_s^+ \rightarrow K^0 \pi^+$

J. Adler, Z. Bai, J. J. Becker, G. T. Blaylock, T. Bolton, J.-C. Brient, J. S. Brown, K. O. Bunnell, M. Burchell, T. H. Burnett, R. E. Cassell, D. Coffman, V. Cook, D. H. Coward, F. DeJongh, D. E. Dorfan, J. Drinkard, G. P. Dubois, G. Eigen, K. F. Einsweiler, B. I. Eisenstein, T. Freese, C. Gatto, G. Gladding, C. Grab, R. P. Hamilton,^(a) J. Hauser, C. A. Heusch, D. G. Hitlin, J. M. Izen, P. C. Kim, L. Köpke, J. Labs, A. Li, W. S. Lockman, U. Mallik, C. G. Matthews, A. I. Mincer, R. Mir, P. M. Mockett, B. Nemati, A. Odian, L. Parrish, R. Partridge, D. Pitman, S. A. Plaetzer, J. D. Richman, M. Roco, H. F. W. Sadrozinski, M. Scarletella, T. L. Schalk, R. H. Schindler, A. Seiden, C. Simopoulos, A. L. Spadafora, I. E. Stockdale, W. Stockhausen, W. Toki, B. Tripsas, F. Villa, M. Z. Wang, S. Wasserbaech, A. Wattenberg, A. J. Weinstein, S. Weseler, H. J. Willutzki, D. Wisinski, W. J. Wisniewski, R. Xu, and Y. Zhu

(The Mark III Collaboration)

California Institute of Technology, Pasadena, California 91125
 University of California at Santa Cruz, Santa Cruz, California 95064
 University of Illinois at Urbana-Champaign, Urbana, Illinois 61801
 University of Iowa, Iowa City, Iowa 52242
 Stanford Linear Accelerator Center, Stanford, California 94309
 University of Washington, Seattle, Washington 98195
 (Received 17 May 1989)

We report the first observation of the decay $D_s^+ \rightarrow \bar{K}^0 K^+$ and a new measurement of the decay $D_s^+ \rightarrow \bar{K}^*(892)^0 K^+$. The data were collected at $\sqrt{s} = 4.14$ GeV with the Mark III detector at the SLAC e^+e^- storage ring SPEAR. We obtain the relative branching fractions $B(D_s^+ \rightarrow \bar{K}^0 K^+)/B(D_s^+ \rightarrow \phi \pi^+) = 0.92 \pm 0.32 \pm 0.20$ and $B(D_s^+ \rightarrow \bar{K}^{*0} K^+)/B(D_s^+ \rightarrow \phi \pi^+) = 0.84 \pm 0.30 \pm 0.22$, using our new determination of $\sigma B(D_s^+ \rightarrow \phi \pi^+)$. A search for the Cabibbo-suppressed decay $D_s^+ \rightarrow K^0 \pi^+$ yields a limit $B(D_s^+ \rightarrow K^0 \pi^+)/B(D_s^+ \rightarrow \phi \pi^+) < 0.21$ at the 90% confidence level.

PACS numbers: 13.25.+m, 14.40.Jz

The weak hadronic decays of D^0 and D^+ mesons have been studied by numerous experiments. Most of these results are understood by QCD-corrected models,¹ which predict an enhancement of the nonleptonic partial widths of both the D^0 and D^+ over the naive spectator model values. No unambiguous evidence for significant exclusive nonspectator processes (W exchange or W annihilation) has yet been observed in D^0 , D^+ , or D_s^+ decays.²⁻⁵ The difference in the D^0 and D^+ total nonleptonic transition rates^{6,7} is thought to be caused by the presence of interference in D^+ decays.^{8,9} The effects of nonspectator diagrams may be understood from further measurements of exclusive charm decay modes. We present herein the first evidence for the decay¹⁰ $D_s^+ \rightarrow \bar{K}^0 K^+$, a new measurement of the decay $D_s^+ \rightarrow \bar{K}^*(892)^0 K^+$, and an upper limit for the decay $D_s^+ \rightarrow K^0 \pi^+$.

The data sample, a total of 6.30 ± 0.46 pb⁻¹, was collected at $\sqrt{s} = 4.14$ GeV with the Mark III detector¹¹ at the SLAC e^+e^- storage ring SPEAR. In this analysis, data from the main drift chamber, the time-of-flight system (TOF), and the dE/dx system are used. At $\sqrt{s} = 4.14$ GeV, D_s^+ mesons are produced predominantly in the reactions¹² (a) $e^+e^- \rightarrow D_s^\pm D_s^{*\mp}$ and (b) $D_s^{*\mp} \rightarrow \gamma D_s^\mp$. The D_s^\pm produced by reaction (a) is referred

to as primary, while that produced by reaction (b) is referred to as secondary. The primary D_s^\pm is produced with a fixed momentum of 0.35 GeV/c, while the secondary D_s^\mp is produced with momentum between 0.18 and 0.47 GeV/c.

The search for $D_s^+ \rightarrow \bar{K}^0 K^+$ is made in the $K_S^0 K^+ \rightarrow \pi^+ \pi^- K^+$ final state. Kaon and pion candidates are selected using particle-identification information from TOF and dE/dx .¹³ Candidate K_S^0 's are formed from all $\pi^+ \pi^-$ combinations in which the reconstructed K_S^0 decay vertex is displaced from the average beam position by at least 3 mm normal to the beam axis. This requirement significantly reduces combinatoric background (Fig. 1), while rejecting only 9% of the $K_S^0 \rightarrow \pi^+ \pi^-$ decays from $D_s^+ \rightarrow \bar{K}^0 K^+$.

Accepted $\pi^+ \pi^- K^+$ combinations are kinematically fitted to the hypothesis $e^+e^- \rightarrow K_S^0 K^+ D_s^{*-}$, where the D_s^{*-} is not reconstructed.¹⁴ Candidates with fit χ^2 confidence level (C.L.) $> 10\%$ are retained, resulting in the $K_S^0 K^+$ mass distribution in Fig. 2(a). An enhancement is observed at the D_s^+ mass. No D_s^+ signal is observed when the imposed recoil mass constraint is placed outside the D_s^* mass region. The fit hypothesis is correct only for decays of primary D_s^+ 's, which are reconstructed with a mass resolution of ~ 5 MeV/c². The fit also

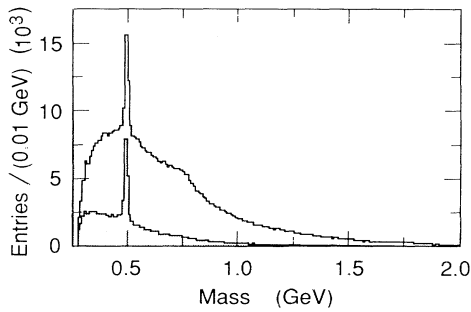


FIG. 1. Inclusive $\pi^+\pi^-$ mass distribution before (unshaded) and after (shaded) the vertex displacement requirement is imposed.

retains secondary decays with $\frac{2}{3}$ of the efficiency for primary decays. These secondary D_s^+ candidates, however, have a broader mass distribution which extends ± 50 MeV/ c^2 about the D_s^+ mass.

The background contribution arising from D^0 and D^+ decays is predicted with a Monte Carlo simulation [shaded histogram in Fig. 2(b)]. At $\sqrt{s}=4.14$ GeV, D mesons are copiously produced in the final states $D^*\bar{D}^*$, $D^*\bar{D}$, and $D\bar{D}$, with production cross sections and decay branching fractions which are well measured in our own data at 3.77 and 4.14 GeV.^{2,6,15,16} No enhancement in the D_s^+ region is predicted to arise from D -meson decays or from other D_s^+ decay modes.

The number of observed $D_s^+ \rightarrow K_S^0 K^+$ decays, 23.3 ± 5.9 , is determined by fitting the mass spectrum in Fig. 2(a). The normalization of the background is allowed to vary and its shape is taken from the unshaded histogram in Fig. 2(b), which shows the sum of the predicted contributions from noncharm continuum events¹⁷ and D decays. The total of these contributions is consistent with the observed number of background entries. The shapes and relative amounts of the primary and secondary signal contributions are also obtained by a Monte Carlo calculation. We assume $B(D_s^{*+} \rightarrow \gamma D_s^+) = 100\%$. The average detection efficiency, including $B(\bar{K}^0 \rightarrow \pi^+\pi^-)$, is 7.8%. This yields the cross section times branching fraction $\sigma B(D_s^+ \rightarrow \bar{K}^0 K^+) = 24 \pm 6 \pm 5$ pb, where $\sigma \equiv \sigma(e^+e^- \rightarrow D_s^+ D_s^{*-} + D_s^- D_s^{*+})$. The systematic error includes the uncertainties in the background shape (13%), the detection efficiency (16%), the integrated luminosity (7%), and the mass of the D_s^{*-} (1%).

To search for the Cabibbo-suppressed decay $D_s^+ \rightarrow K^0 \pi^+$, a similar procedure is followed.¹⁸ The resulting $K_S^0 \pi^+$ mass spectrum appears in Fig. 3(a). Monte Carlo signal and background shapes are determined as in the $D_s^+ \rightarrow \bar{K}^0 K^+$ analysis. The predicted number of D and continuum entries agrees with the observed spectrum [Fig. 3(b)]. A 90%-C.L. upper limit of 3.8 signal events is obtained by integrating the likelihood function. Allowing for efficiency (9.5%) and increasing the limit by the systematic uncertainty (18%) yields $\sigma B(D_s^+ \rightarrow K^0 \pi^+) < 3.7$ pb (90% C.L.).

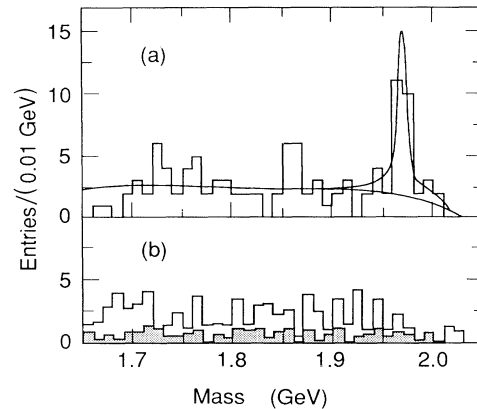


FIG. 2. (a) $K_S^0 K^+$ mass distribution after kinematic fit. (b) Background distributions predicted by a Monte Carlo simulation, normalized to integrated luminosity of the data set. The shaded histogram shows the contribution from $D^*\bar{D}^*$, $D^*\bar{D}$, and $D\bar{D}$ events; the unshaded histogram gives the total for these final states and noncharm continuum events.

The $D_s^+ \rightarrow \bar{K}^*(892)^0 K^+$ decay is studied in the $K^+ K^- \pi^+$ final state. In the inclusive $K^- \pi^+$ mass spectrum (Fig. 4), a \bar{K}^{*0} signal is observed with the expected mass and width. A one-constraint kinematic fit to the hypothesis $e^+e^- \rightarrow K^+ K^- \pi^+ D_s^{*-}$ is performed for each $K^+ K^- \pi^+$ combination. The $\bar{K}^{*0} K^+$ mode is selected by requiring the fitted $K^- \pi^+$ mass to be within 75 MeV/ c^2 of the nominal \bar{K}^{*0} mass. For the reaction $D_s^+ \rightarrow \bar{K}^{*0} K^+$, $\bar{K}^{*0} \rightarrow K^- \pi^+$, the polar angle θ_π of the π^+ in the \bar{K}^{*0} helicity frame is expected to have a $\cos^2 \theta_\pi$ distribution. The requirement $|\cos \theta_\pi| > 0.3$ is imposed to improve the signal-to-background ratio. The resulting $\bar{K}^{*0} K^+$ mass distribution [Fig. 5(a)] shows a D_s^+ signal. The validity of the $D_s^+ \rightarrow \bar{K}^{*0} K^+$ signal is checked by examining \bar{K}^{*0} sidebands and by varying the recoil mass constraint. No peak is observed at the D_s^+ mass in ei-

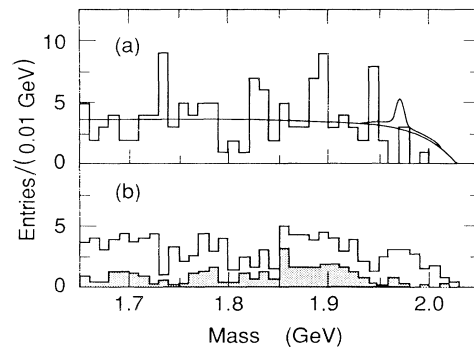


FIG. 3. (a) $K_S^0 \pi^+$ mass distribution after kinematic fit. The curve represents the 90%-C.L. upper limit on the number of signal events. (b) Monte Carlo background distributions: D events (shaded) and the sum of D and noncharm continuum events (unshaded).

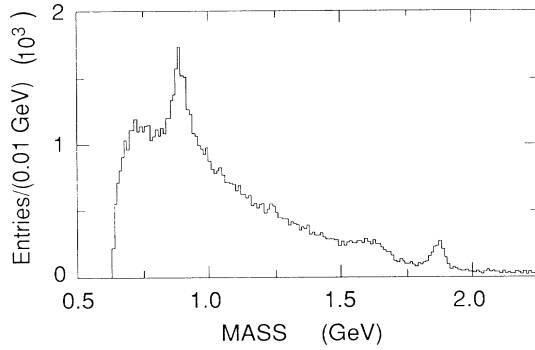


FIG. 4. Inclusive $K^-\pi^+$ mass distribution. The enhancements in the high mass region result from $D \rightarrow \bar{K}\pi\pi$ and $D \rightarrow \bar{K}\pi$.

ther case.

The mass spectrum in Fig. 5(a) is fitted by the procedure used in the $\bar{K}^0 K^+$ analysis. The predicted background contribution from D decays and noncharm continuum events [Fig. 5(b)] is again consistent with the observed total background. The signal contains 23.8 ± 6.3 entries. A subtraction is made for two sources of background which produce enhancements at or near the D_s^+ mass: $D^+ \rightarrow \bar{K}^{*0}\pi^+$ (0.8 ± 0.6 event¹⁵) and nonresonant $D_s^+ \rightarrow K^+ K^-\pi^+$ (1.8 ± 0.8 events¹⁹). The decay $D_s^+ \rightarrow \phi\pi^+$ is excluded by the \bar{K}^{*0} requirement on the $K^-\pi^+$ mass. The detection efficiency for $D_s^+ \rightarrow \bar{K}^{*0}K^+$, including $B(\bar{K}^{*0} \rightarrow K^-\pi^+)$, is 7.8%, yielding $\sigma B(D_s^+ \rightarrow \bar{K}^{*0}K^+) = 22 \pm 6 \pm 6$ pb. The systematic error accounts for the uncertainties in the shape of the smooth background (21%), the Monte Carlo efficiency (14%), the integrated luminosity (7%), and the subtraction of background from the signal peak (5%).

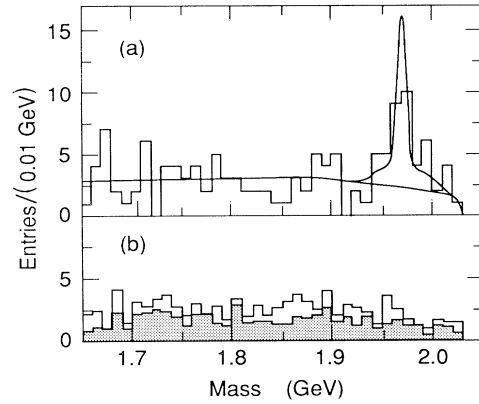


FIG. 5. (a) $\bar{K}^{*0}K^+$ mass distribution after kinematic fit, requiring $|\cos\theta_x| > 0.3$. (b) Monte Carlo background distributions: D events (shaded) and the sum of D and noncharm continuum events (unshaded).

To obtain more precise measurements of D_s^+ decay modes relative to $\phi\pi^+$, we have improved our determination¹² of $\sigma B(D_s^+ \rightarrow \phi\pi^+)$ by using the same kinematic fitting technique. The systematic uncertainty on the reconstruction efficiency has been reduced to 14% by further study of D decays in the same data set. The result is $\sigma B(D_s^+ \rightarrow \phi\pi^+) = 26 \pm 6 \pm 5$ pb. Our measured relative branching fractions are given in Table I. The $\bar{K}^{*0}K^+$ result is consistent with previous measurements.¹⁹⁻²²

The predictions of a factorization calculation⁹ (model 1), a QCD sum-rule analysis²³ (model 2), and a model with final-state interactions²⁴ (model 3) are compared with the observed relative branching fractions in Table I.

TABLE I. Relative D_s^+ branching fractions.

	Experiment	Model 1 ^a	Model 2 ^b	Model 3 ^c
$\frac{B(D_s^+ \rightarrow \bar{K}^0 K^+)}{B(D_s^+ \rightarrow \phi\pi^+)}$	$0.92 \pm 0.32 \pm 0.20^d$	0.47	0.43	
	$0.84 \pm 0.30 \pm 0.22^d$			
	$0.87 \pm 0.13 \pm 0.05^e$			
$\frac{B(D_s^+ \rightarrow \bar{K}^{*0}\pi^+)}{B(D_s^+ \rightarrow \phi\pi^+)}$	$0.89 \pm 0.32 \pm 0.13^f$	0.55	0.74	
	0.93 ± 0.37^g			
	1.44 ± 0.37^h			
$\frac{B(D_s^+ \rightarrow K^0\pi^+)}{B(D_s^+ \rightarrow \bar{K}^0 K^+)}$	< 0.22 (90% C.L.) ^d	0.20		0.11 to 0.22
$\frac{B(D_s^+ \rightarrow K^0\pi^+)}{B(D_s^+ \rightarrow \phi\pi^+)}$	< 0.21 (90% C.L.) ^d	0.09		

^a Reference 9.

^b Reference 23.

^c Reference 24.

^d This experiment.

^e Reference 19.

^f Reference 20.

^g Reference 21.

^h Reference 22.

The decays $D_s^+ \rightarrow \bar{K}^0 K^+$, $\bar{K}^{*0} K^+$, and $K^0 \pi^+$ may proceed through spectator or annihilation processes. The measurements of $D_s^+ \rightarrow \bar{K}^0 K^+$ and $D_s^+ \rightarrow \bar{K}^{*0} K^+$ relative to $D_s^+ \rightarrow \phi \pi^+$ (a spectator decay) are higher than the theoretical predictions.²⁵ However, uncertainties in these predictions preclude a definitive statement concerning the relative importance of spectator and nonspectator processes.

We gratefully acknowledge the dedicated efforts of the SPEAR staff. One of us (G.E.) wishes to thank the A. von Humboldt Foundation for support. This work was supported by the Department of Energy, under Contracts No. DE-AC03-76SF00515, No. DE-AC02-76ER01195, No. DE-AC03-81ER40050, No. DE-AC02-87ER40318, No. DE-AM03-76SF00034, and by the National Science Foundation.

^(a)Deceased.

¹For a review, see M. A. Shifman, in *International Symposium on Lepton and Photon Interactions*, edited by W. Bartel and R. Rückl (North-Holland, Amsterdam, 1987).

²R. M. Baltrusaitis *et al.*, Phys. Rev. Lett. **56**, 2136 (1986).

³J. Adler *et al.*, Phys. Rev. Lett. **60**, 1375 (1988).

⁴H. Albrecht *et al.*, Phys. Lett. B **195**, 102 (1987).

⁵J. C. Anjos *et al.*, Phys. Rev. Lett. **62**, 125 (1989).

⁶R. M. Baltrusaitis *et al.*, Phys. Rev. Lett. **54**, 1976 (1984); **55**, 638(E) (1985).

⁷J. C. Anjos *et al.*, Phys. Rev. D **37**, 2391 (1988).

⁸B. Guberina *et al.*, Phys. Lett. **89B**, 111 (1979); Y. Koide, Phys. Rev. D **20**, 1739 (1979); G. Altarelli and L. Maiani, Phys. Lett. **118B**, 414 (1982).

⁹M. Bauer, B. Stech, and M. Wirbel, Z. Phys. C **34**, 103 (1987). Revised values of $a_1=1.2$ and $a_2=-0.5$ are taken from B. Stech, Heidelberg University Report No. HD-THEP-87-18, 1987 (unpublished).

¹⁰We adopt the convention that reference to a state also implies reference to its charge conjugate.

¹¹D. Bernstein *et al.*, Nucl. Instrum. Methods Phys. Res.,

Sect. A **226**, 301 (1984).

¹²G. T. Blaylock *et al.*, Phys. Rev. Lett. **58**, 2171 (1987).

¹³Kaon candidates are required to have a usable TOF measurement t , with $|t - t_K|/\sigma_K < |t - t_\pi|/\sigma_\pi$, where t_π and t_K are the predicted π and K times and σ_π, σ_K are the uncertainties on the time differences. The TOF system provides π - K separation of $> 2\sigma$ over the relevant range of K^\pm momenta ($p < 1.1$ GeV/c). All tracks are accepted as pion candidates, except when the measured TOF is inconsistent with the π hypothesis. Further background rejection is obtained from dE/dx measurements for pion candidates not having TOF information.

¹⁴A D_s^* mass of 2.109 GeV/c² is used (Ref. 12).

¹⁵J. Adler *et al.*, Phys. Lett. B **196**, 107 (1987).

¹⁶R. M. Baltrusaitis *et al.*, Phys. Rev. Lett. **55**, 150 (1985); **56**, 2140 (1986); J. Adler *et al.*, Phys. Rev. Lett. **60**, 89 (1988); Phys. Lett. B **208**, 152 (1988).

¹⁷We use the Jetset 6.2 event generator [T. Sjöstrand, Comput. Phys. Commun. **39**, 347 (1986)].

¹⁸The pion *not* from the K_S^0 decay is required to have TOF identification analogous to the kaons in Ref. 13.

¹⁹We use the measurement of $B(D_s^+ \rightarrow K^+ K^- \pi^+)_{NR}/B(D_s^+ \rightarrow \phi \pi^+)$ from J. C. Anjos *et al.*, Phys. Rev. Lett. **60**, 897 (1988).

²⁰S. Barlag *et al.*, CERN Report No. CERN-EP/88-103, 1988 (unpublished).

²¹M. P. Alvarez *et al.*, CERN Report No. CERN-EP/88-148, 1988 (unpublished).

²²H. Albrecht *et al.*, Phys. Lett. B **179**, 398 (1986).

²³B. Yu. Blok and M. A. Shifman, Yad. Fiz. **45**, 211 (1987); **45**, 478 (1987); **45**, 841 (1987); **46**, 1310 (1987) [Sov. J. Nucl. Phys. **45**, 135 (1987); **45**, 301 (1987); **45**, 522 (1987); **46**, 767 (1987)].

²⁴A. N. Kamal and R. C. Verma, Phys. Rev. D **35**, 3515 (1987); **36**, 3527(E) (1987). The predictions are derived with $\delta^{*K}=100^\circ$. The parameter p in this calculation is constrained by our limit to values < 0.5 .

²⁵Although the model 1 predictions shown do not include final-state interactions, it is interesting to note that better agreement with the data is achieved for the ratios shown in Table I by using $|a_1/a_2| \sim 1.8$. The uncertainty in this ratio is 25% (Ref. 9), so this represents a 1σ deviation from the nominal value of $|a_1/a_2| = 2.4$.